Iranian Journal of Materials Science and Engineering, Vol. 19, Number 3, September 2022
RESEARCH PAPER

High Photocatalytic Performance of Zno/Fe_3O_4 and Tio_2/Fe_3O_4 Nanostructures Thin Films against Methylene Blue Dye under Visible Light Irradiation

M. J. Kadhim[1,*], Fatima Allawi[2], M. A. Mahdi[1], Sami Najah Abaas[1]

* *marooj2013@gmail.com*

[1] Department of Physics, College of Science, University of Basrah, Basrah, Iraq
[2] Department of Chemistry, College of Science, University Kufa, Najaf, Iraq

Received: September 2021 **Revised: December 2021** **Accepted: February 2022**

DOI: 10.22068/ijmse.2461

Abstract: *The present study was aimed to assess the effect of replacing copper in the brake pad with potassium titanate platelet (PTP) and ceramic fiber (CF). Chase dynamometer tests were conducted to compare a brake pad's tribological behavior when PTP and CF are added to the composition with that of the copper-bearing pad. The results indicated that PTP and CF demonstrated promising outcomes such as a stable coefficient of friction (COF), lower wear rate, and better heat resistance in copper-free friction composite. Scanning electron microscope (SEM/EDS) analysis was conducted to investigate the role of main elements such as Ti, Fe, K, O, and C on the formation of contact plateaus of friction composites. PTP maintained both continuous contact and smooth friction braking application of a brake pad. The uniform distribution of Ti on the wear track on the worn surface depicts the role of PTP in stabilizing the friction film formation.*

Keywords: *copper-free, potassium titanate, ceramic fiber, brake pad, friction materials*

1. INTRODUCTION

In recent years, pollutants such as organic material were increased in the water as a results to the great expansion of the industry and the spread of factories on the banks of rivers that led to cause a serious environmental problems leading to appear various diseases because of their bio-accumulate in the body of living organisms and capability to be persistent in the environment. Removing these pollutants from the water is very important, but by using environmentally safe and effective methods. Degradation of these pollutants from water can be done using photocatalyst metal oxide materials such as TiO_2 and ZnO which have high removal ability for polluted toxic organic material with simple and low-cost processes [1, 2]. Metal oxides materilas in general have a wide band gap in the near-UV region, strong oxidation ability, non-toxic as well as stable chemically [2, 3]. ZnO and TiO_2 can be used to remove and degrade organic dyes like methylene blue (MB) to CO_2 and H_2O under UV light irradiation but the use of ultraviolet light is undesirable because of the harm it causes to humans [4, 5]. Therefore, various modifications such as metal and non-metal doping, and coupling with other semiconductors and noble metals have been used to enhance the visible light absorption of metal oxide [5, 6]. When metal oxide photocatalyst combine with a magnetic compound such as FeO, Fe_2O_3, and Fe_3O_4, the photocatalytic activity for degradation organic dyes will happen under visible light [7]. The Fe_3O_4 compound has attracted more attention from researchers because of it's the good ability for using as a photocatalytic material. A.V. Tajareh et al. [8] used Fe_3O_4 to enhance photocatalytic hybrid of prepared TiO_2/Fe_3O_4 and TiO_2/Fe_3O_4/MWCNT nanostructures and obtained a high photodegradation rate and better recyclability. Further, C. Karunakaran et al. [9] prepared Fe_3O_4/ZnO nanostructure as a photocatalysts and they found that the compound appeared effective photodegradation of organic pollutants under UV and visible light irradiation [9].

In the present work, ZnO and TiO_2 nanostructures thin films were prepared via chemical bath deposition (CBD) method while ZnO/Fe_3O_4 and TiO_2/Fe_3O_4 nanostructures thin films were synthesized by casting Fe_3O_4 nanoparticles onto the grown ZnO and TiO_2 thin films. The photocatalytic activity against MB dye of all prepared samples were investigated using a pH of 10 under visible light exposure.

[DOI: 10.22068/ijmse.2461]

2. MATERIALS AND METHODS

2.1. Preparation of ZnO NRs and TiO_2 nanostructured thin films

The ZnO nanostructures thin films were prepared onto glass substrates via the chemical bath deposition method as described in our previous work [4] while TiO_2 nanocrystalline thin films were prepared by CBD method onto glass substrates using the same parameters that used by Salman et al. [10]. However, briefly substrates were cleaned by hydrochloric acid (HCl), 2-propanol, ethanol subsequently using ultrasound cleaner. Substrates were vertically immersed in the beaker contains precursor of 4 ml of titanium (III) chloride ($TiCl_3$) solution, 50 ml deionized water (DI), and 0.1 M of urea [NH_2CONH_2] that was added to adjust the pH of the solution to 0.5. After stirring at room temperature for 1 h, a homogeneous violet solution was obtained. The solution temperature is fixed at 55°C for 3 h and after finishing, substrates were removed from the beaker, cleaned by distilled water (DW), and annealed at 350°C for 1h to enhance the crystallinity of prepared samples.

2.2. Preparation of Fe_3O_4 nanoparticles

The Fe_3O_4 nanoparticles were prepared using a facile hydrothermal method. The $FeCl_2$ and $FeCl_3$ with a molar ratio of 1:2 were dissolved in 50 ml of deionized water (DI) and then a drop wise of 1M sodium hydroxide (NaOH) was added to the solution under continuous stirring to adjust pH value at 10. The mixture was transferred to a 70 ml of Teflon-lined stainless-steel autoclave that was fixed inside the oven at a temperature of 200°C for 4hr. After the preparation process was completed, the autoclave was taken out from the oven and left to cool naturally. A dark red precipitate was obtained indicting to form Fe_3O_4 nanoparticles. The obtained product was washed by DI water and ethanol for three times using a centrifuge. Further, the prepared Fe_3O_4 nanoparticles were annealed at 550°C for 2 h to enhance the crystallinity.

2.3. Synthesis of TiO_2/Fe_3O_4 and ZnO/Fe_3O_4 nanostructured thin films

A 0.1 g of Fe_3O_4 nanoparticles were suspended in 100 ml of DI and the solution was sonicated for 10 min with the power of 800 Watt using sonicator type Tefic Biotech Co., Limited 10 min. The prepared solution is cast on ZnO nanorods and TiO_2 nanostrucures thin films to prepare both ZnO/Fe_3O_4 and TiO_2/Fe_3O_4 nanostrucures thin films. Prepared samples were annealed at 350°C for 1h to enhance interfacing contact between the core (ZnO& TiO_2) and shell (Fe_3O_4) layer.

2.4. Samles characterization

Surface morphology of prepared ZnO/Fe_3O_4 and TiO_2/Fe_3O_4 nanostrucures thin films grown onto glass substrates through the CBD method was investigated through Field-Emission Scanning Electron Microscope (FESEM) type FEI Nova NanoSEM 450. Crystalline structure of prepared samples was studied by X-ray diffraction method using XPertPro (MPD) (PanAlytical-The Netherland). All measurments were done at Nanotechnology lab., Department of Physics, College of Science, University of Basrah.

2.5. Photocatalytic Study

Photocatalytic activity of ZnO/Fe_3O_4 and TiO_2/Fe_3O_4 nanostrucures thin a film was investigated using an aqueous of 200 ml DW contains 0.001 g of Methylene Blue (MB) dye. Prepared ZnO/Fe_3O_4 and TiO_2/Fe_3O_4 nano-strucures thin films were placed in a beaker contains 40 ml of MB dye solution and illuminated by 82 mW/m^2 of visible light. The degradation ratio of MB day solution is estimated using various values of pH, temperature, and time of exposure. The degradation rate of MB dye was calculated using below formula [11]**:**

$$Degradation\ rate(\%) = \frac{A_\circ - A}{A_\circ} \times 100\% \quad (1)$$

Where A_o, A are the absorbance value before and after exposure by visible light for several minutes, respectively. However, absorbance spectra of MB dye that catalyzed by ZnO, ZnO/Fe_3O_4, TiO_2, and TiO_2/Fe_3O_4 nanostrucures thin film were measured by spectrometer type (PASCO SPECTROMETER PS-2600).

The pH value of MB dye solution was fixed at 10 by adding some drops of NaOH solution. The pH was control the type of surface charge of the photocatalytic where the surface charge of photocatalytic will be positive in the acidic medium and negative in the basal medium. Degradation kinetics (k) of the MB dye can be described using the first-order Langmuir equation represented by [3]:

$$C = C_o e^{-kt} \quad (2)$$

Where t is the time of the reaction, C_o is the initial

[DOI: 10.22068/ijmse.2461]

concentration of MB dye, C is the concentration after exposure, and k is the first order constant of the degradation reaction. The concentration is calculated according to Beer–Lambert's law [12]:

$$A = \varepsilon C l \quad (3)$$

Where A is absorbance, ε is representing of molar absorptivity was taken of value from our previous study [4], and l is the UV light path length (1 cm).

3. RESULTS AND DISCUSSION

3.1. Surface morphology

Figure 1 shows the FESEM image of ZnO/Fe_3O_4 and TiO_2/Fe_3O_4 nanostrucures thin films grown onto glass substrates through the CBD method.

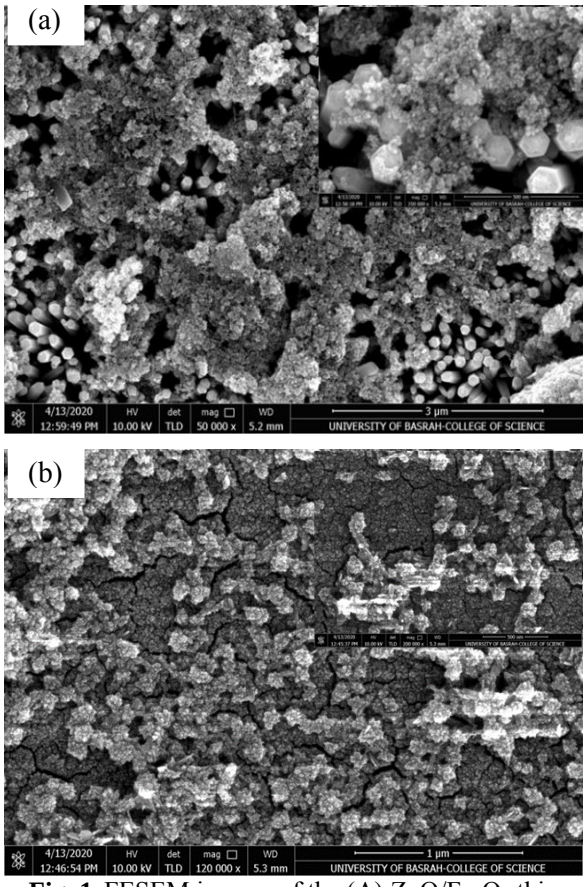

Fig. 1. FESEM images of the (A) ZnO/Fe_3O_4 thin film and (B) TiO_2/Fe_3O_4 thin film.

The ZnO thin film were grown as a nanorods (NRs) with a diameter range of 10–130 nm while the Fe_3O_4 were grown as a nanoparticles (NPs) covered the surface of ZnO NRs as shown in Fig.1A. Figure 1B shows the FESEM image of TiO_2/Fe_3O_4 nanostructures thin film grown onto a glass. Figure 2 shows the distribution of the Fe_3O_4 NPs diameters using ImageJ software and found that the diameter range was 8–59 nm with dominated particles dimeter between 10 and 30 nm.

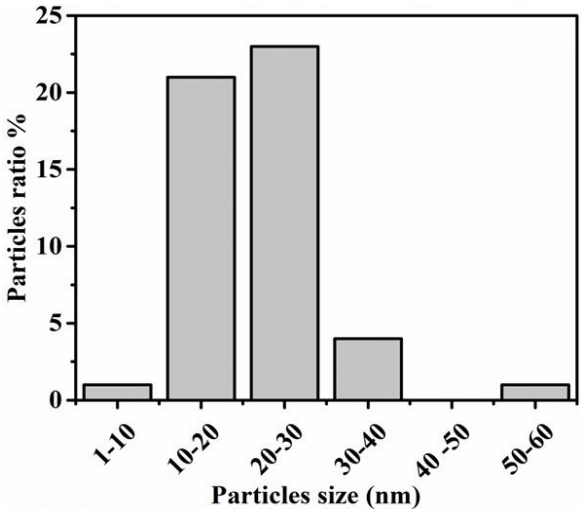

Fig. 2. Statistical distribution of the Fe_3O_4 NPs.

3.2. Crystalline structure

Figure 3A shows XRD pattern of Fe_3O_4 NPs that appeared diffraction peaks at 2θ of 30.10°, 35.57°, 43.20°, and 57.17° that corresponding to crystalline planes of (220), (311), (400), and (511), respectively of Face Center Cubic (FCC) of Fe_3O_4 according to standard XRD database (JCPDS card no. 19-0629). However, the XRD results confirmed that no other phase of other compounds was formed. Furthermore, the crystal size of Fe_3O_4 was 22 nm which is calculated using the Scherrer equation [13]. Figure 3B shows XRD pattern of ZnO/Fe_3O_4 nanostructures thin films that appears XRD peaks at 2θ of 31.78°, 34.43°, 36.24°, 47.52°, and 56.56° that related to crystalline planes of (100), (002), (101), (102), and (110), respectively of hexagonal (wurtzite) structure of ZnO (JCPDS card No., 36-1451) [14, 15]. Figure 3C shows the XRD pattern of TiO_2/Fe_2O_3 nanostructures and observed XRD peaks at 2θ of 25.17°, 38.31°, 47.782°, and 54.753° which corresponding to planes of (011), (110), (020), and (121), respectively of anatase TiO_2 compound (JCPDS file No. 96-900-4143 and 96-900-8216) [16]. However, the low XRD intensity indicates to poor crystallinity of TiO_2 as well as the absence the diffraction peaks that corresponding to Fe_3O_4 is due to the low ratio in sample.

[DOI: 10.22068/ijmse.2461]

3.3. Photocatalytic degradation of MB dye

Figure 4 shows the relationship between photodegradation rate of MB dye and irradiation time for ZnO, ZnO/Fe_3O_4, TiO_2, and TiO_2/Fe_3O_4 nanostructures thin film and noted the photodegradation rate of ZnO NRs is 28% at 240 min while for ZnO/Fe_3O_4 nanostructures thin film at 150 min is 87% and reached to 100% after exposure by visible light for 180 min. Moreover, the photodegradation rate of TiO_2 nanostructures thin film is 26% at 240 min while TiO_2/Fe_3O_4 nanostructures thin film appears photo-degradation rate of 82% at the same time of the irradiation.

Although, the base medium of the MB solution increases formation of hydroxyl radicals OH that leads to increase photocatalysis process [16, 17]. The obtained results show the ZnO/Fe_3O_4 and TiO_2/Fe_3O_4 nanostructures thin films appeared photocatalysts higher than the photocatalysis that aobtained by ZnO and TiO_2 thin films because of the synergic effect between metal oxides material and magnetic material of Fe_3O_4. The Fe^{3+} ions in Fe_3O_4 will work to prevent recombination charge carriers in metal oxide catalysts that could be led to improve the photocatalysis process [17–19]. Y. Lei et al. got a photodegradation rate of 18.9% obtained by Fe_3O_4/ZnO nanostructure at 180 min of illumination [20] while T. Tan et al. obtained a photodegradation rate of 87.9% for TiO_2/Fe_3O_4 nanostructure [21]. The degradation mechanism of ZnO/Fe_3O_4 depending of absorbing photons by both ZnO and Fe_3O_4 and form the electron/hole pairs. However, ZnO and Fe_3O_4 have a positions of conduction bands (−0.45 eV and −0.58 eV vs NHE) and valence bands (+ 2.75 eV and + 0.99 eV vs NHE), respectively [22].

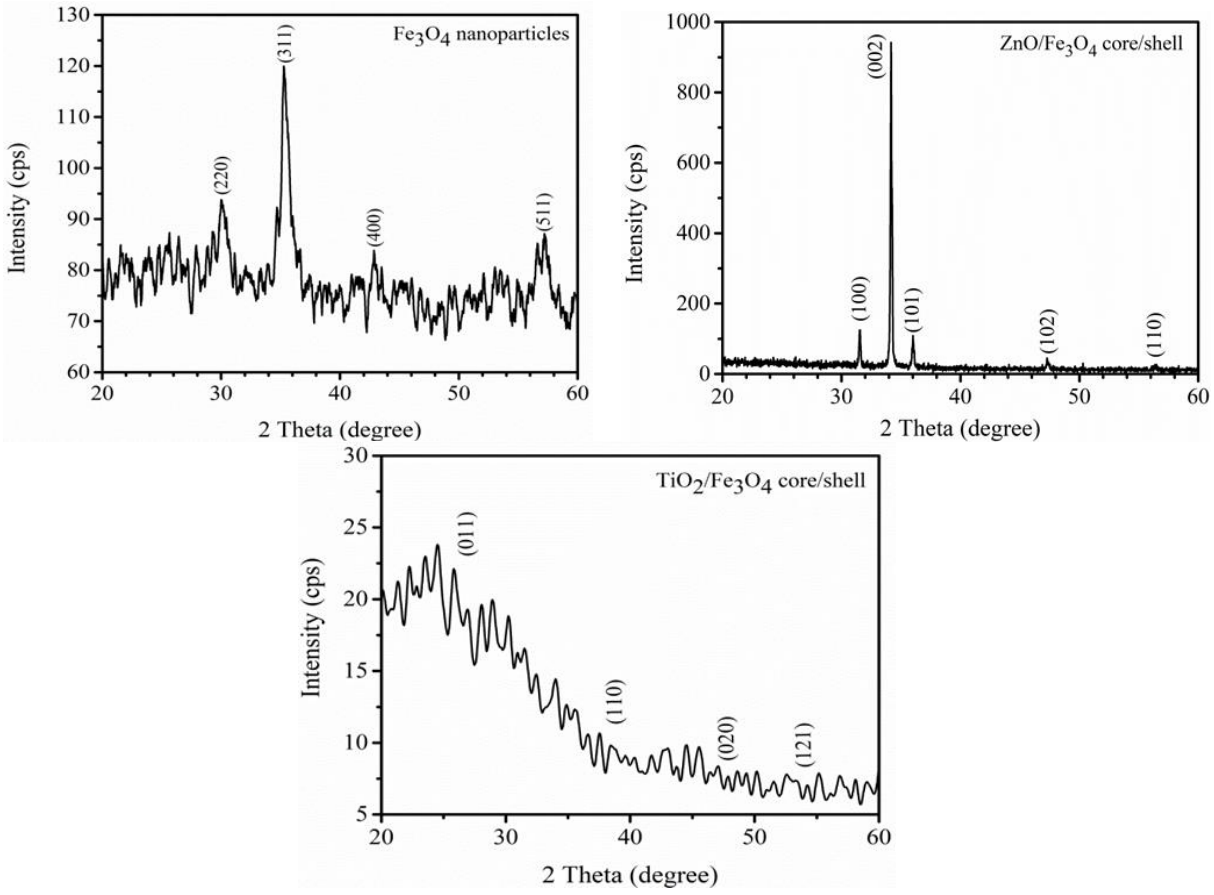

Fig. 3. XRD patterns of Fe_3O_4 NPs, ZnO/Fe_3O_4 thin film, and TiO_2/Fe_3O_4 thin film.

[DOI: 10.22068/ijmse.2461]

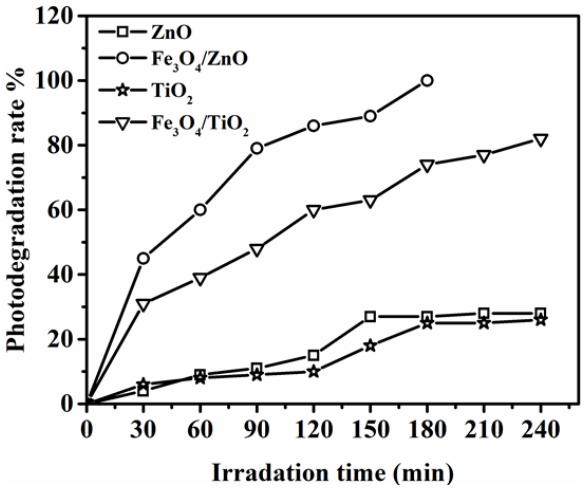

Fig. 4. MB dye photodegradation rate vs. illumination time for ZnO, TiO_2, ZnO/Fe_3O_4, and TiO_2/Fe_3O_4 nanocrystalline thin films.

Therefore, the electrons of the conduction band (CB) of Fe_3O_4 would migrate to the ZnO while holes at the valence band (VB) of Fe_3O_4 would remain that led to reduce the electron/hole recombination. Thus, the photocatalytic activity of the Fe_3O_4/ZnO is better than of pure ZnO. Then, the OH^- present in the aqueous solution will capture by the hole of the valence band to form highly reactive OH radical. Finally, the dye molecules attacked by the radical to decompose into simple products as shown by the following reaction steps [23]:

$$Fe_3O_4/ZnO \rightarrow Fe_3O_4/ZnO(h^+) + Fe_3O_4/ZnO(e^-) \quad (1)$$

$$Fe_3O_4/ZnO(e^-) + (O_2) \rightarrow O_2^- \quad (2)$$

$$Fe_3O_4/ZnO(h^+) + H_2O \rightarrow OH^{\cdot} + H^+ \quad (3)$$

$$H_2O + O_2^- \rightarrow 2OH \quad (4)$$

$$OH + MB \rightarrow \text{degradation products} \quad (5)$$

The enhancement of the photocatalytic activity of Fe_3O_4/TiO_2 nanoparticles can be interpreted by energy level theory: the energy level of Fe^{3+}/Fe^{2+} closes to the energy level of TiO_2's conduction band, and the energy level of Fe^{3+}/Fe^{4+} closes to the energy level of TiO_2's valence band. Thus, the Fe^{3+} ions that dissolved from Fe_3O_4 nanoparticles can act as a capture electron position as well as work as a hole capture position that led to decrease the electron–hole pair recombination of TiO_2 [24]. Figure 5A shows the C/C_o plot vs. irradiation time of ZnO, ZnO/Fe_3O_4, TiO_2, and TiO_2/Fe_3O_4 nanostructures thin film catalyzed MB dye and found that the concentration of MB dye was decreased when irradiation time was increased. Figure 5B shows the variation of $-\ln(C/C_o)$ vs. irradiation time for the prepared catalysts nanostructures thin films. Furthermore, the kinetic rate of degradation of MB dye was calculated from the slope and it was 0.00156 min^{-1} and 0.0141min^{-1} for ZnO and ZnO/Fe_3O_4 nanostructures thin films, respectively. The kinetic rate of TiO_2 and TiO_2/Fe_3O_4 nanostructures thin films was 9.9333 x 10^{-4} min^{-1} and 0.0068 min^{-1}, respectively. Increasing the kinetic rate value led to convert the reaction kinetics and the equilibrium properties of the adsorbent process [25].

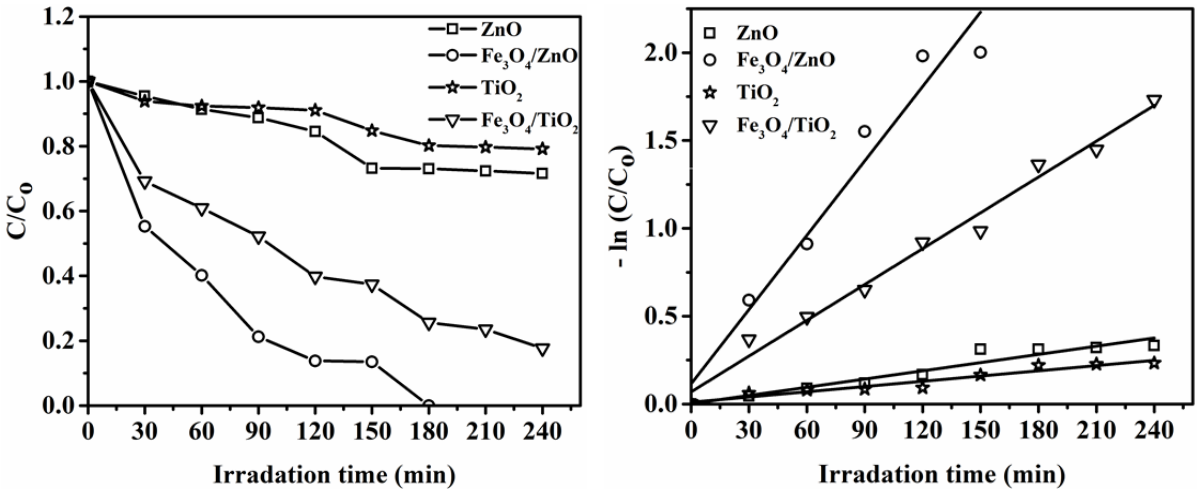

Fig. 5. (A) Kinetics of photocatalytic degradation with irradiation time (B) Variation of $-\ln(C/C_o)$ with irradiation time under visible light for ZnO, TiO_2, ZnO/Fe_3O_4, TiO_2/Fe_3O_4 nanostructured thin films.

[DOI: 10.22068/ijmse.2461]

Table 1. Photocatalytic activity of different Fe_3O_4 nanostructures

Photocatalysts	Morphology	Photodegradation rate %	Irradiation of time (min)	Dye type	K(min^{-1})	Reference
Fe_3O_4/ZnO	Core-Shell NPs	18.9	180	MB	0.00958	[20]
Fe_3O_4/ZnO	Core-Shell NPs	73	60	MO	0.00221	[26]
Fe_3O_4-ZnO	Core-Shell NPs	94	120	MB	$208x10^{-4}$	[15]
TiO_2/Fe_3O_4	NPs	80.8	120	MB	--	[27]
TiO_2	NPs	19.04	240	MO	--	[8]
TiO_2/Fe_3O_4		19.02			--	
ZnO/Fe_3O_4	Nanostuctur	100	180	MB	0.01411	Current work
TiO_2/Fe_3O_4	Nanosrtuctur	82	240	MB	0.0068	Current work

4. CONCLUSIONS

ZnO NRs thin films and TiO_2 nanostructuers thin films were grown onto glass substrates by the CBD method. The ZnO/Fe_3O_4 and TiO_2/Fe_3O_4 thin films were prepared by drop casting of Fe_3O_4 NPs onto the grown ZnO and TiO_2 nanostructuers thin films. The photocatalytic activity against MB dye was investigated at pH value of 10 under visible light irradiation. The photodegradation rate of MB was increased when used as-prepared ZnO/Fe_3O_4 and TiO_2/Fe_3O_4 nanostrcuters thin films photocatalysts with increasing irradiation time. The enhancement of the photocatalytic activity of the as-prepared ZnO/Fe_3O_4 and TiO_2/Fe_3O_4 nanostrcuters thin films could be due to the absorbance of light by Fe_3O_4 nanoparticles in the visible region. Moreover, the Fe^{+3} could act to prevent recombination carriers in metal oxide (ZnO) catalysts which can lead to improved photocatalytic activity.

REFERENCES

[1] P. Goyal, S. Chakraborty, S. K. Misra, Multifunctional Fe_3O_4-ZnO nanocomposites for environmental remediation applications, Environ. Nanotechnology, Monit. Manag., 10, 2018, 28–35. doi: 10.1016/j.enmm.2018.03.003.

[2] H. S. Lim, J. S. Lee, S. Lee, Y. S. Kang, Y. K. Sun, K. Do Suh, Walnut-like ZnO@Zn_2TiO_4 multicore-shell submicron spheres with a thin carbon layer: Fine synthesis, facile structural control and solar light photocatalytic application, Acta Mater., 122, 2017, 287–297. doi: 10.1016/j.actamat.2016.09.031.

[3] Q. Feng, S. Li, W. Ma, H.-J. Fan, X. Wan, Y. Lei, Z. Chen, J. Yang, B. Qin, Synthesis and characterization of Fe_3O_4/ZnO-GO nanocomposites with improved photocatalytic degradation methyl orange under visible light irradiation, J. Alloys Compd., 737, 2018, 197–206. doi: 10.1016/j.jallcom.2017.12.070.

[4] M. J. Kadhim, M. A. Mahdi, J. J. Hassan, Influence of pH on the photocatalytic activity of ZnO nanorods, Mater. Int., 2, 2020, 0064–0072. doi: 10.1007/s10854-016-4284-0.

[5] A. Ziashahabi, M. Prato, Z. Dang, R. Poursalehi, N. Naseri, The effect of silver oxidation on the photocatalytic activity of Ag/ZnO hybrid plasmonic/metal-oxide nanostructures under visible light and in the dark, Sci. Rep., 9, 2019, 1–12. doi: 10.1038/s41598-019-48075-7.

[6] M. J. Kadhim, M. Mahdi, J. J. Hassan, A. S. Al-Asadi, Photocatalytic activity and photoelectrochemical properties of Ag/ZnO core/shell nanorods under low-intensity white light irradiation, Nanotechnology, 32, 2021, 195706. doi.org/10.1088/1361-6528/abe3b3

[7] S. B. Atla, W.-R. Lin, T.-C. Chien, M.-J. Tseng, J.-C. Shu, C.-C. Chen, C.-Y.Chen, Fabrication of Fe_3O_4/ZnO magnetite core shell and its application in photocatalysis using sunlight, Mater. Chem. Phys., 216, 2018, 380–386. doi: 10.1016/

[DOI: 10.22068/ijmse.2461]

j.matchemphys.2018.06.02.

[8] A. V. Tajareh, H. Ganjidoust, B. Ayati, Synthesis of TiO_2/Fe_3O_4/MWCNT Magnetic and Reusable Nanocomposite with High Photocatalytic Performance in the Removal of Colored Combinations from Water, J. Water Environ. Nanotechnol., 4, 2019, 198–212. doi: 10.22090/jwent.2019.03.003.

[9] C. Karunakaran, P. Vinayagamoorthy, J. Jayabharathi, Nonquenching of Charge Carriers by Fe_3O_4 Core in Fe_3O_4 /ZnO Nanosheet Photocatalyst, Langmuir, 30, 2014, 15031–15039. doi: 10.1021/la5039409.

[10] A. M. Selman, Z. Hassan, M. Husham, Structural and photoluminescence studies of rutile TiO_2 nanorods prepared by chemical bath deposition method on Si substrates at different pH values, Measurement, 56, 2014, 155–162.

[11] S. Raghu, C. W. Lee, S. Chellammal, S. Palanichamy, C. A. Basha, Evaluation of electrochemical oxidation techniques for degradation of dye effluents—A comparative approach, J. Hazard. Mater., 171, 2009 748–754. doi: https://doi.org/10.1016/j.jhazmat.2009.06.063.

[12] M. B. Gholivand, J. B. Ghasemi, S. Saaidpour, A. Mohajeri, Spectrophotometric study of the effects of surfactants and ethanol on the acidity constants of fluorescein, Spectrochim. Acta Part A Mol. Biomol. Spectrosc., 71, 2008, 1158–1165.

[13] M. A. Mahdi, Z. Hassan, S. S. Ng, J. J. Hassan, S. K. M. Bakhori, Structural and optical properties of nanocrystalline CdS thin films prepared using microwave-assisted chemical bath deposition, Thin Solid Films, 520, 2012, 3477–3484, doi: 10.1016/j.tsf.2011.12.059.

[14] S. M. Lam, J. A. Quek, J. C. Sin, Surfactant-free synthesis of ZnO micro/nanoflowers with efficient photocatalytic antibacterial performance, Mater. Lett., 195, 2017, 34–36. doi: 10.1016/j.matlet.2017.02.084.

[15] S. Ghanbarnezhad, S. Baghshahi, A. Nemati, M. Mahmoodi, Preparation, magnetic properties, and photocatalytic performance under natural daylight irradiation of Fe_3O_4-ZnO core/shell nanoparticles designed on reduced GO platelet, Mater. Sci. Semicond. Process., 72, 2017, 85–92. doi: 10.1016/j.mssp.2017.09.015.

[16] A. H. Kianfar, M. A. Arayesh, Synthesis, characterization and investigation of photocatalytic and catalytic applications of Fe_3O_4/TiO_2/CuO nanoparticles for degradation of MB and reduction of nitrophenols, J. Environ. Chem. Eng., 8, 2020, 103640. doi: 10.1016/j.jece.2019.103640.

[17] L. B. Reuterglrdh, M. Langphasuk, photocatalytic decolourization of reactive azo dye: a comparison between TiO_2 and cds photocatalysis, Chemosphere, 35, 1997, 585–596.

[18] S. Dehghan, A. Jonidi, M. Farzadkia, A. Esra, Visible-light-driven photocatalytic degradation of Metalaxyl by reduced graphene oxide/Fe_3O_4/ZnO ternary nanohybrid : In fl uential factors , mechanism and toxicity bioassay, J. Photochem. Photobiol. A Chem., 375, 2019, 280–292. doi: 10.1016/j.jphotochem.2019.01.024.

[19] L. I. Yuxiang, Z. Mei, G. U. O. Min, W. Xidong, Preparation and properties of a nano TiO_2/Fe_3O_4 composite superparamagnetic photocatalyst, RARE Met., 28, 2009, 423–427. doi: 10.1007/s12598-009-0082-7.

[20] Y. Lei, J. Ding, P. Yu, G. He, Y. Chen, H. Chen, Low-temperature preparation of magnetically separable Fe_3O_4@ZnO-RGO for high-performance removal of methylene blue in visible light, J. Alloys Compd., 821, 2020, 153366. doi: 10.1016/j.jallcom.2019.153366.

[21] T. Tan, P. Khiew, W. Chiu, C. Chia, Magnetised photocatalyst TiO_2/Fe_3O_4 nanocomposite capable to photodegrade organic dye, Mater. Sci. Eng., 744, 2020, 012021. doi: 10.1088/1757-899X/744/1/012021.

[22] B. Zhu, G. Jiang, Y. Lv, F. Liu, J. Sun, Photocatalytic degradation of polyacrylamide by rGO@Fe_3O_4/Cu_2O@ZnO magnetic recyclable composites, Mater. Sci. Semicond. Process., 131, 2021, 105841.

[DOI: 10.22068/ijmse.2461]

doi: 10.1016/j.mssp.2021.105841.
[23] R. Elshypany, H. Selim, K. Zakaria, A. H. Moustafa, S. A. Sadeek, S.I. Sharaa, P. Raynaud, A. A. Nada, Elaboration of Fe_3O_4/ZnO nanocomposite with highly performance photocatalytic activity for degradation methylene blue under visible light irradiation, Environ. Technol. Innov., 23, 2021, 101710. doi: 10.1016/j.eti.2021.101710.
[24] J. Zhan, H. Zhang, G. Zhu, Magnetic photocatalysts of cenospheres coated with Fe_3O_4/TiO_2 core/shell nanoparticles decorated with Ag nanopartilces, Ceram. Int., 40, 2014, 8547–8559. doi: 10.1016/j.ceramint.2014.01.069.
[25] M. Do˘gan, Y. O.¨zdemir, M. Alkan, Adsorption kinetics and mechanism of cationic methyl violet and methylene blue dyes onto sepiolite, Dye. Pigment., 75, 2007, 701–713. doi: 10.1016/j.dyepig.2006.07.023.
[26] J. Xia, A. Wang, X. Liu, Z. Su, Preparation and characterization of bifunctional, Fe_3O_4/ZnO nanocomposites and their use as photocatalysts, Appl. Surf. Sci., 257, 2011, 9724–9732. doi: 10.1016/j.apsusc.2011.05.114.
[27] L. Gnanasekaran, R. Hemamalini, S. Rajendran, J. Qin, M. L. Yola, N. Atar, F.Gracia, Nanosized Fe_3O_4 incorporated on a TiO_2 surface for the enhanced photocatalytic degradation of organic pollutants, J. Mol. Liq., 287, 2019, 2–8. doi: 10.1016/j.molliq.2019.110967.

[DOI: 10.22068/ijmse.2461]